# SHOCK TUBE EXPERIMENTS ON FLAME PROPAGATION REGIMES AND CRITICAL CONDITIONS FOR FLAME ACCELERATION AND DETONATION TRANSITION FOR HYDROGEN-AIR MIXTURES AT CRYOGENIC TEMPERATURES

**M. Kuznetsov[1]*, A. Denkevits[1], A. Veser[2], A. Friedrich[2], G. Necker[2], T. Jordan[1]**
**[1] Karlsruhe Institute of Technology, Kaiserstrasse 12, Karlsruhe 76131, Germany,**
**[2] Pro-Science GmbH, Parkstrasse 9, Ettlingen 76275, Germany**
***E-mail: kuznetsov@kit.edu**

## ABSTRACT

A series of more than 100 experiments with hydrogen-air mixtures at cryogenic temperatures have been performed in a shock tube in the frame of the PRESLHY project. A wide range of hydrogen concentrations from 8 to 60%H2 in the shock tube of the length of 5 m and 50 mm id was tested at cryogenic temperatures from 80 to 130K at ambient pressure. Flame propagation regimes were investigated for all hydrogen compositions in the shock tube at three different blockage ratios (BR) 0, 0.3 and 0.6 as a function of initial temperature. Pressure sensors and InGaAs-photodiodes have been applied to monitor the flame and shock propagation velocity of the process. The experiments at ambient pressure and temperature were conducted as the reference data for cryogenic experiments. A critical expansion ratio for an effective flame acceleration to the speed of sound was experimentally found at cryogenic temperatures. The detonability criterion for smooth and obstructed channels was used to evaluate the detonation cell sizes at cryogenic temperatures as well. The main peculiarities of cryogenic combustion with respect to the safety assessment were that the maximum combustion pressure was several times higher compared to ambient temperature and the run-up-distance to detonation was several times shorter independent of lower chemical reactivity at cryogenic conditions.

## 1.0 INTRODUCTION

Within the flammability limits, three typical combustion regimes can be distinguished for gaseous mixtures. These include slow subsonic deflagrations ($v < c_r$ - flame velocity v is less than the speed of sound in reactants $c_r$), fast supersonic flame ($c_r < v < c_p$ - flame velocity is less than the sound speed in products $c_p$, but more than the sound speed in reactants), and detonation ($v = D_{CJ}$, Chapman-Jouguet velocity). All possible regimes and characteristic pressure profiles based on paper [1] are shown in Figure 1 for hydrogen-air mixtures at initial pressure of 1 bar.

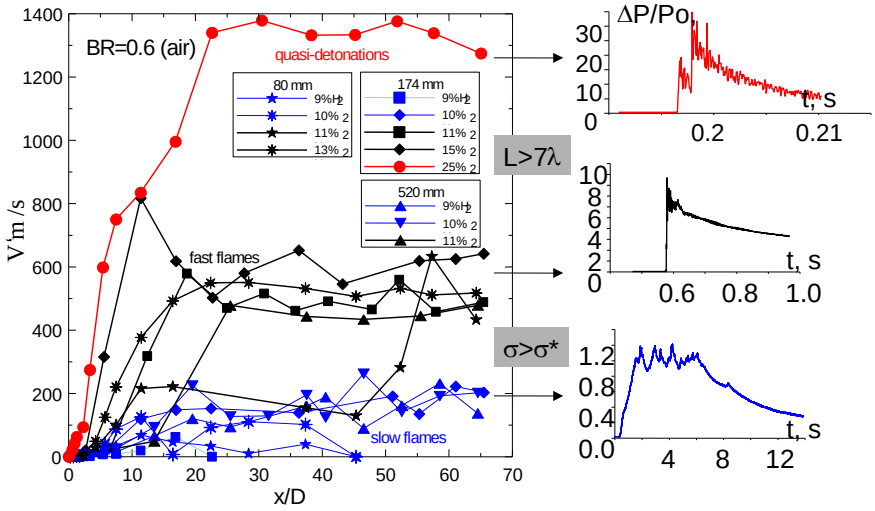


Figure 1. Combustion regimes for hydrogen-air mixtures in a tube geometry [1-2].

As it was suggested by Dorofeev and co-authors [1-2], the critical expansion rate σ* and 7λ - criteria can be used as potentials for strong flame acceleration and detonation onset, respectively. Mixtures with the expansion rate σ above the critical value σ* can effectively accelerate to the speed of sound and then detonate, if the detonation criteria L > 7λ is satisfied (L is the characteristic size of the combustible domain; λ is the detonation cell size). The mixtures with σ < σ* cannot accelerate to the speed of sound and only subsonic combustion regimes may occur. Characteristic combustion pressure depends on flame propagation velocity and can be changed from 1-2 bar for slow combustion, to 6-8 bar for sonic deflagration and 20-40 bar for detonation at initial pressure 1 bar (Figure 1).

The critical expansion ratio σ* is a function of dimensionless integral scale as Peclet number Pe = $L_T/\delta$ ($L_T$ - turbulent length scale, δ -laminar flame thickness) and Zeldovich number β (β = $E_a(T_b-T_u)/T_b^2$). The critical Peclet number Pe > 100 was experimentally found to be required for the strong flame acceleration and to exclude a local flame extinction due to heat losses [1]. The Peclet number lower than 100 may result in critical expansion ratio increase. The critical expansion ratio σ* decreases with initial temperature $T_u$ increase and overall energy activation $E_a$ decrease. Since adiabatic combustion temperature $T_b$ is almost independent of the initial temperature $T_u$, the critical expansion ratio is only a function of the energy activation and temperature [1]:

$$\sigma^* = 9.0\cdot10^{-6}x^3 - 0.0019x^2 + 0.1807x + .2314, \qquad (1)$$

where $x=E_a/RT_u$. Assuming a constant activation energy $E_a$=7500K for hydrogen-air mixtures in wide range of temperatures and concentrations, an extrapolation to cryogenic temperatures gives the values of the critical expansion ratio σ* = 7.89 at T = 80K. For T = 100K, the σ* = 6.9 which roughly corresponds to 7-8%H2 in air. The assumption about the constant activation energy in wide range of temperatures and concentrations is very strong and may lead to over-conservative results by shifting the critical concentration to leaner hydrogen - air mixtures that requires stronger measures to the hydrogen safety.

Figure 2 shows an extrapolation of critical expansion ratio to cryogenic temperatures without an effect of the energy activation. Far extrapolation to low temperatures gives the values of critical expansion ratio σ* and critical hydrogen concentration leading to an effective flame acceleration to the speed of sound at different initial temperatures: σ* = 8.5 (9.6% H2) at 100K and σ* = 10.7 (9.1%H2) at 78K.

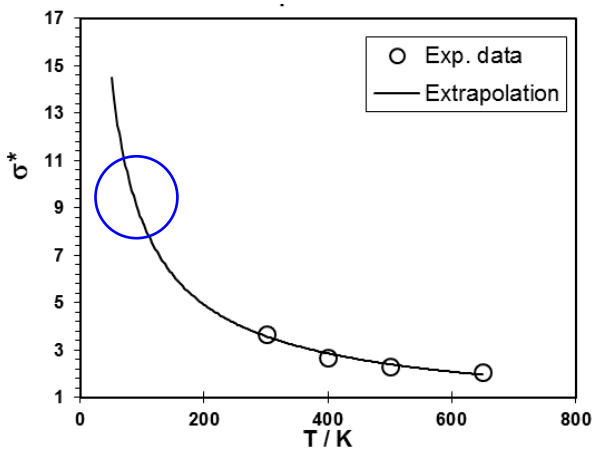


Figure 2. Critical expansion ratio $\sigma$ versus initial temperature $T_u$ for hydrogen – air mixtures. The critical points at elevated temperatures are taken from [1].

The previous extrapolation looks not enough confident because it is too far for such nonlinear dependence. The dependence of critical expansion ratio vs. Zeldovich number looks more linear (Figure 3). Assuming the constant activation energy, an effect of initial temperature on the critical

expansion ratio can also be evaluated. Extrapolation to cryogenic temperature 80K leads to Zeldovich number increase to β = 11. According to the correlation in Figure 3, it corresponds to the critical expansion ratio of about σ* = 8, which in turn corresponds to 7%H2/air mixture at 80K. However, there is a highly requested need to experimentally check the theoretical prediction of critical expansion ratio at cryogenic temperatures. Another reason is that independent of the higher energy of combustion at cryogenic temperatures caused by three times higher density, the chemical reactivity of such compositions as 7% H2/air at low temperatures might be too low even to be ignited.

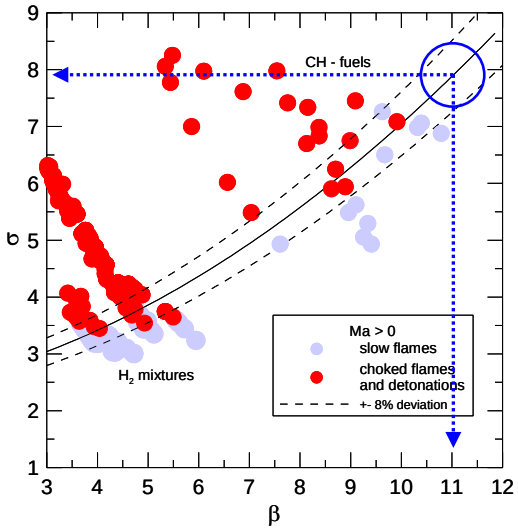


Figure 3. Critical expansion ratios for possible development of fast flames in obstructed channels vs. Zeldovich number [1]. Blue circle indicates the area of interest extrapolated to cryogenic temperatures

The σ - criterion gives a potential for flame acceleration to the speed of sound but it needs some distance to accelerate the flame to the speed of sound. Figure 4 demonstrates the dependence of run-up-distance to sonic deflagration or detonation calculated according to papers [1-4] for a tube with different roughness or blockage ratio. The dependence is based on papers [3-4] and uses the formula that takes into account the roughness or blockage of the channel and chemical reactivity of the mixture [4]. The tubes with a roughness of 5 and 50 μm can be assumed as smooth ones. A simplified rough value for run-up distance to detonation in smooth channel sounds as $X_D$=500λ [3]. Figure 4 clearly shows the efficiency of obstructions with respect to the shortening of the distance $X_D$ to sonic flame or detonation. For instance, the only stoichiometric hydrogen-air at T = 293K can be accelerated to detonation within a 5-m tube length. To detonate the less reactive mixture of 20%$H_2$ we need a run-up distance $X_D$=5.1 m for BR = 0.1, $X_D$=4.1 m for BR = 0.3, and $X_D$=3.4 m for BR = 0.6.

The detonations may only occur if the flame reaches the speed of sound. Then, the critical condition when the characteristic size of the channel (tube diameter d, for instance) L > λ/π for a smooth channel or L > 7λ for an obstructed channel should be satisfied [2]. This means that the characteristic size of the combustible system should exceed seven cell sizes for detonation onset inside of the obstructed channel. In particular, the condition L >7λ can be transformed to d > λ for BR=0.3 and d > 3λ for BR=0.6 [5-6]. If one of the abovementioned detonation conditions is not satisfied, a sonic deflagration in an obstructed tube can be stabilized as a stationary chocked flame that propagates with the speed of sound in combustion products [1-4].

There is a lack of experimental data on detonation cell size at cryogenic and reduced (lower than the ambient) temperatures in mixtures containing the hydrogen. The only one reference is known regarding the cryogenic temperature conditions. Paper [7] gives detonation cell sizes for stoichiometric hydrogen oxygen mixtures at 123K and different initial pressures.

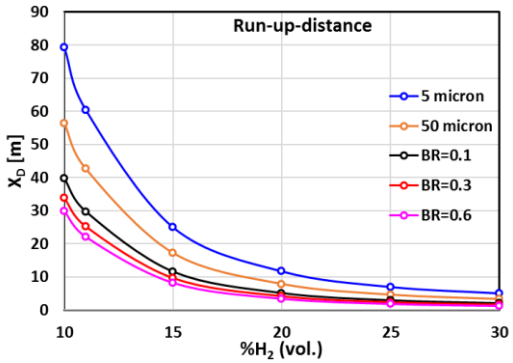


Figure 4. Calculations for run-up-distances $X_D$ for rough/smooth and obstructed tubes.

For hydrogen-air mixtures we only have experimental data on the influence of elevated initial temperature on detonation cell size (see Figure 5). In general, in accordance with referred data [8-10] the detonation cell size is increasing with temperature decrease. These referred data cover relatively narrow range of temperatures (278-373K) for hydrogen-air mixture with $\phi = 0.5$. In general, we can extrapolate these data to lower temperatures but not far. We use the CELL_H2 for more accurate detonation cell size predictions [11]. The code CELL_H2 uses detail chemical kinetics and takes into account multidimensional detonation cell structure. The code is verified in wide range of elevated pressures and temperatures and mixture compositions. It demonstrates very good capability within the range 278-373K. The problem is to apply the CELL_H2 code below 200 K due to the lack of available thermodynamic and kinetic data. Figure 5 and Figure 6 show that CELL_H2 code demonstrates very good reliability for elevated and normal temperatures [8-10]. However, the code gives strong under-prediction at cryogenic temperatures (Figure 6) compared to the experimental data [7]. However, both figures demonstrate that until the maximum of the dependence $\lambda(T)$ and even to the beginning of the decay at temperatures lower than 273K the code gives proper results which can be linearly extrapolated even to 100K. Because of very far extrapolation we strongly need additional experimental data on detonation cell sizes at cryogenic temperatures.

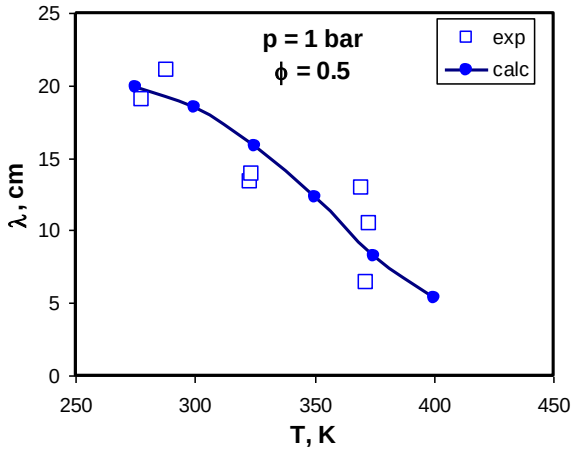


Figure 5. Comparison of calculated and experimental data for detonation cell size of hydrogen-air mixtures at different temperatures [8-9].

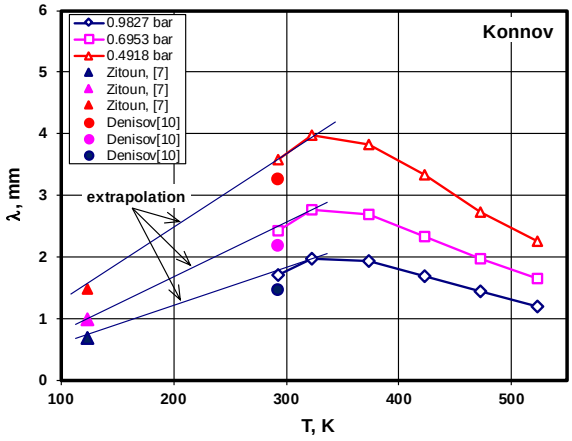


Figure 6. Comparison of calculated (empty points) and experimental data (solid points) for detonation cell size of hydrogen-oxygen mixtures at different temperatures and pressures [7,10]

The objective of current work is to evaluate the critical conditions for flame acceleration (FA) and detonation transition (DT) for hydrogen-air mixtures at cryogenic temperatures, possibly in the presence of condensed oxygen and nitrogen. The data are required for safety analysis to evaluate the strongest possible combustion pressure and safety distances for $LH_2$ explosions.

## 2.0 EXPERIMENTAL SETUP AND PROCEDURE

The facility consists of a stainless steel tube 5-m long with an outer diameter of 73 mm and an inner diameter of 54 mm. To provide the cryogenic temperatures, the tube was exposed in a metal basin filled with liquid nitrogen (LN2). The tube and the basin were supported by metal frame structure (Figure 7). A basin made of stainless steel insulated with Styrofoam provided the cooling. The cooling degree was planned by varying amount of $LN_2$.

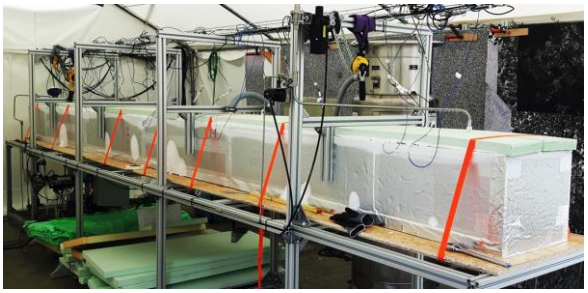

Figure 7. Cryo-shock tube inside a bath of LN2 with supporting structure.

The experimental procedure was different for ambient and cryogenic initial temperatures. The scheme of the setup for the gas management is shown in Figure 8. Only the "Cryo valve" is exposed to $LN_2$ prior to the cryogenic experiments. All other valves and devices are at ambient temperature. All valves have pneumatic actuators. There was no pure gas-cooling loop in the $LN_2$ bath, because of the possibility for $LO_2$ condensation at such temperature. To extract water, the tube was first purged with dry compressed $N_2$. Then, the tube was evacuated down to < 1 mbar. The bath was filled with liquid N2. The temperature of the tube wall was controlled at 3 outside points along the tube with thermocouples clamped to the wall. A test mixture was prepared with 2 Mass Flow Controllers (MFC, Bronkhorst), one for H2 and another for synthetic air (N2+O2). A H2-sensor checks the H2 concentration in this mixture. During this step, the prepared mixture was released to the air through the bypass at the inlet side. When the mixture in preparation had an acceptable concentration, the valve to the tube was opened and the tube was filled with the required test composition. The mixture was flowed through a pipeline loop below the LN2 level to cool the mixture down before entering the tube. Then, the mixture was kept flowing through the tube until the concentration at the outlet side reached a stable value. When the gas temperature inside and mixture pressure were stabilized, all the valves were closed to be ready for the test. Finally, the mixture was ignited triggering the data acquisition.

A standard automotive spark plug was used for ignition together with a matching HV generator (Bosch type). For some mixtures enriched with hydrogen or approaching the flammability limits a glow plug with a heating element was activated. The problem, in this case, was that the mixture in the vicinity of the igniter was heated up because of the longer induction time to ignition and also the ignition moment was not exactly known as for the spark plug. The number of repetitions was limited, because the cooled tube acts as a cold trap. It was nearly impossible to remove the condensed combustion products by pumping them at temperatures below 183 K.

The experiments on hydrogen flame propagation have been conducted in a tube geometry with 3 different blockage ratios BR = 0, 30 and 60%. 0% of blockage simply means a smooth tube without obstacles. The blockages 30 and 60% are provided by a set of metal rings fully filled the tube length and spaced by the tube diameter. Stainless steel rings of appropriate cross-sections on threaded bars lead to blockage ratios of 30 % or 60 %. The blockage ratio is defined as follows: $BR = 1 - d^2/D^2$, where d is the internal diameter of the obstacle ring; D is the inner tube diameter. The distance between the rings equal to the tube diameter is fixed by nuts on three bars. The obstacles (Figure 9) are 10 mm thick and their exact mid-to-mid distance was 50 mm. All ports and sensors are placed midway in between the obstacle positions.

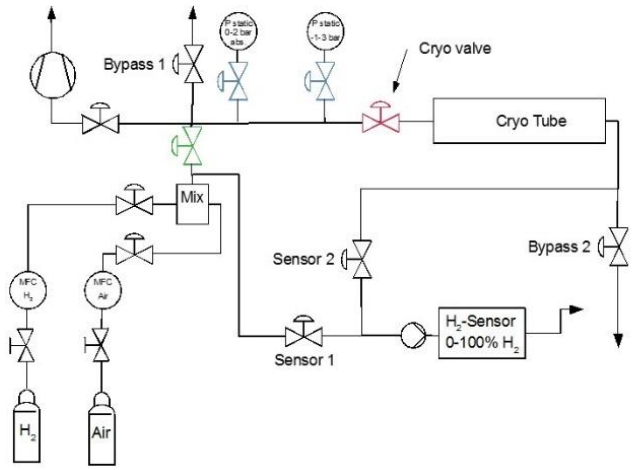


Figure 8. Low temperature gas filling system.


Figure 9. Obstacles grid elements.

Along the tube, 52 ports in 16 cross sections (Figure 10) have been fabricated for 13 pressure sensors and photodiode assemblies. The distances from the ignition flange to each sensor are listed in Figure 10. Two types of dynamic pressure sensors suitable for cryo-temperatures with $p_{max}$ = 6.9 bar (PCB 116B) and 345 bar (PCB 112A05) were used. The pressure sensors were mounted flush to the inner tube wall through the adaptors provided by the sensor manufacturer. Due to the low hydrogen flame emissivity, an InGaAs photodiode was chosen as the light sensor. Because the photo sensor material does not withstand the low temperature, the light signal was guided by a polymer optical fiber to the sensor outside of the $LN_2$ bath. An adaptor with a quartz glass plate between two PTFE rings provided the vacuum-tight sealing to the interior of the tube. The other end of the light guide was fixed to the photodiode by adhesive tape.

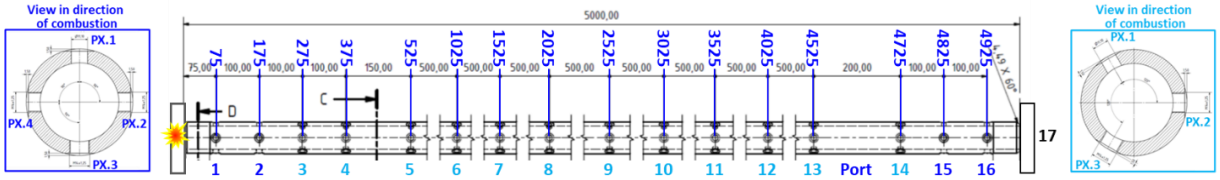


Figure 10. The tube and port locations.

To monitor the cooling process, four thermocouples (type K) were placed at the outer tube surface, and two thermocouples were inside the tube, just at the inner surface. Their distances from the front flange were 22.5 cm, 102.5 cm, 103 cm, 227 cm, 378 cm and 472.5 cm respectively. In preliminary experiments, the thermocouples were exposed at ambient and LN2 boiling temperature of 77K. Then, a linear correlation is used to adjust the measured temperature to the real one. By the averaging, it yields the linear correction with an RMS = ± 0.18 K:

$$T_r\,[K] = 1.1013 * T_m\,[K] - 31.024 \qquad (2)$$

where $T_r$ and $T_m$ are the real and measured temperatures in Kelvin. An actual initial temperature for each test was assumed to be as an average for all six thermocouples.

## 3.0 MAIN RESULTS AND DISCUSSION

### 3.1 Warm tests (T=293K).

A series of reference tests at ambient pressure and temperature and different blockages of the tube 0, 30 and 60% was conducted to check the well known criteria for flame acceleration and DDT [1-2] for the same tube geometry as for the forthcoming cryogenic tests. The experiments with a smooth tube (BR=0) cover hydrogen-air mixtures in the range 8-60%. That was mainly relatively slow subsonic deflagration registered because of longer run-up-distance (RUD) to detonation than the length of the tube L=5 m. The only stoichiometric mixture was able to detonate at the shock wave reflection on the far end flange. Figure 11 presents distance – time diagrams for subsonic deflagration (left) and sonic deflagration and detonation transition (right) as a sequence of signal – time histories for sensors vertically located in accordance with their position along the tube. The horizontal axis is the time scale. The slope of the line between two characteristic peaks belonged to two different sensors gives the velocity of a certain process (flame or shock propagation).

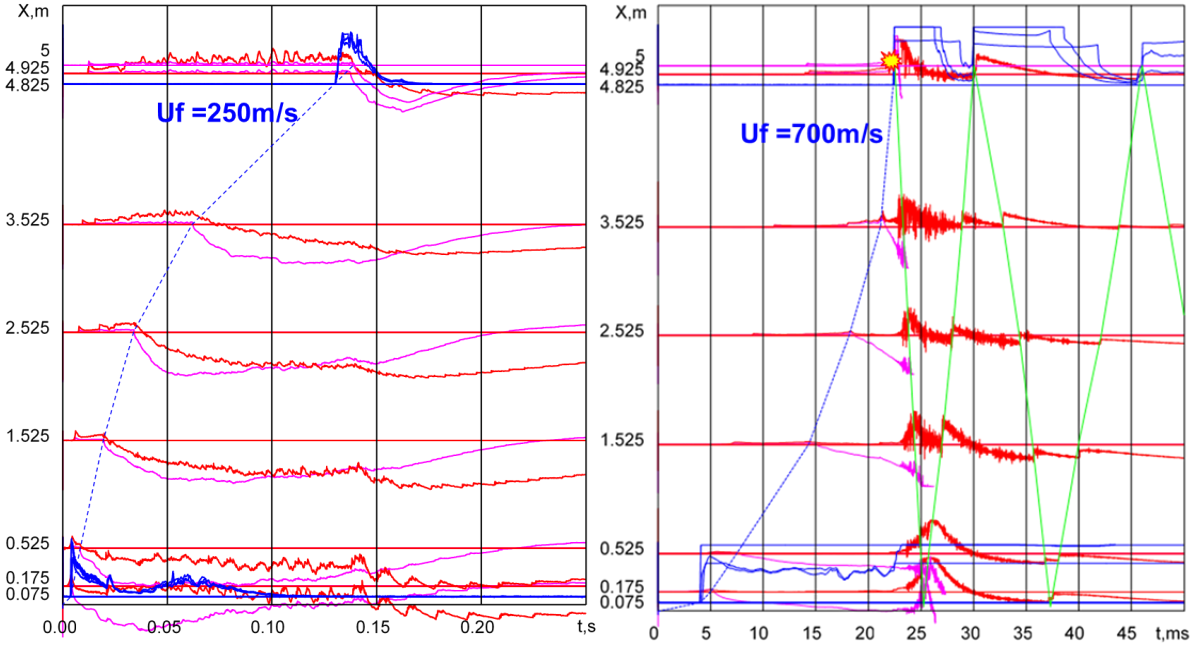


Figure 11. Distance-time diagram for subsonic deflagration, 45%H2 (left) and for detonation transition, 30%H2 (right): flame trajectory (blue dotted line); shock wave trajectory (green line);light signal (blue solid line); pressure signal (red and pink solid lines). The star corresponds to DDT point.

According to paper [3], the run-up distance to detonation in a smooth channel should be 500 times larger than the detonation cell size $x_D = 500\ \lambda$. For 45%H2-mixture (Figure 11, left), the flame accelerates very slowly and, since the run-up distance to fast sonic flame was larger than the tube length, the detonation did not occur: $x_D = 500\ \lambda = 8400$ mm > L=5000 mm. This happens independent of the high mixture reactivity and small enough detonation size $\lambda = 16.8$ mm sufficient for detonation propagation in a smooth tube ($\lambda < \pi D = 170$ mm). For stoichiometric hydrogen-air mixture (Figure 11, right), the flame successfully accelerates to supersonic velocity with a relatively strong shock wave which is able to initiate the detonation being reflected at the far end flange. The run-up-distance to detonation $x_D = 500\ \lambda = 5000$ mm (where $\lambda$=10 mm for stoichiometric hydrogen-air) exactly fits to the length of the tube L=5000mm.

With the obstructions, we can experimentally evaluate the critical expansion ratio σ* for an efficient flame acceleration to the speed of sound because obstacles reduce the run-up-distance almost three times compared to smooth tube. Characteristic combustion pressure and flame speed are measured in each experiment. In presence of obstacles, the flame continuously accelerates until a steady-state velocity is established. For both obstacles (BR=0.3-0.6), for hydrogen concentration above 11%H2 (σ=3.77), characteristic flame velocity above the speed of sound (blue dotted line in Figure 12, right) and characteristic combustion pressure above the adiabatic combustion pressure ΔPicc (red dotted line in Figure 12, left) is etablished. For more reactive mixtures, the velocity approaches the detonation velocity D_CJ, when the detonability criteria are satisfied. The detonation cell size of test mixture should be larger than the orifice diameter, λ < d=45.2 mm for BR = 0.3 or λ < d/3=9.5 mm for BR = 0.6 according to papers [2,5-6,14]. In reality, it corresponds to more than 19.5%H2 for BR=0.3 or 30%H2 for BR=0.6. Figure 12 confirms the critical expansion ratio σ*=3.75 for hydrogen-air mixtures at ambient conditions in a tube with BR=0.3. The same threshold was found for BR=0.6.

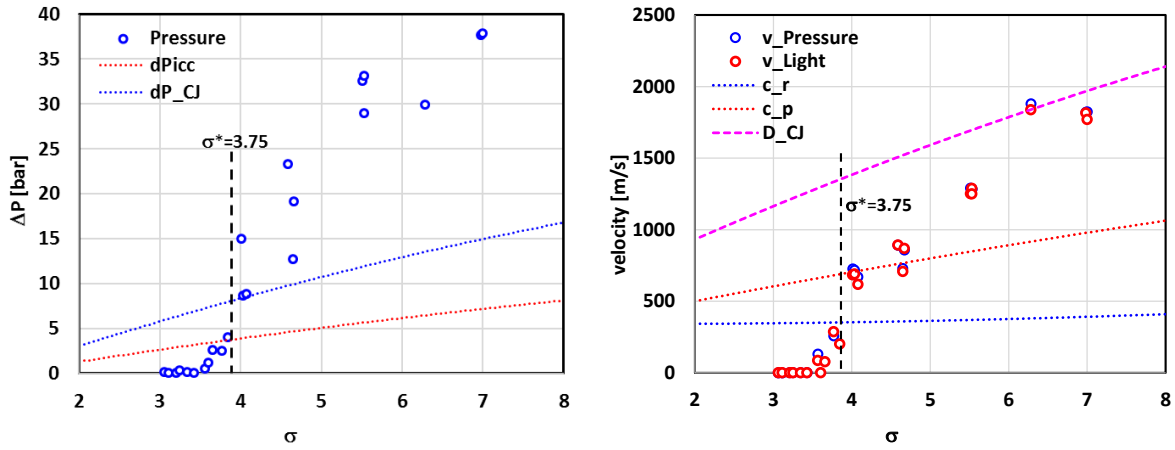


Figure 12. Characteristic pressure (left) and flame velocity (right) in obstructed tube (BR=0.3) as function of expansion ratio at ambient conditions: black dashed line is a cut-off line at σ*=3.75.

### 3.2 Cryogenic tests (T=90-130K)

The tube is cooled down in the basin surrounded the tube with $LN_2$, and the experiments are conducted during the warm-up phase. It takes about 2 hours to cool the tube down from ambient to the test temperature 90-130 K. Temperature uniformity along the tube is monitored by six thermocouples. We suppose the temperature of test mixture is established as an average before the test.

Typical x-t diagrams for cryogenic hydrogen combustion in a smooth tube (BR=0) are presented in Figure 13 for chocked sonic flame (19.6%H2), detonation (45%H2) and again sonic chocked flame (50%H2). For the first time, it was discovered a stationary supersonic flame propagationin a channel without obstacles. For hydrogen-air mixtures of 16% - 17%H2, a stationary flame front coupled with shock wave propagates with characteristic velocity of the order of speed of sound in combustion products Uf=600-800 m/s (Mach number M=3). It can be classified as a chocked flame supported by spatial problems and energy losses. If the detonability of tested mixture would be larger, then the detonation for mixtures above 20% can occur. Since the critical condition for detonation propagation in a smoot channel is d > λ/π, we can assume the detonation cell size λ < π d = 170 mm for mixtures of more than 20%H2. In contrary, for non-detonable mixtures with 16 and 17%H2 the detonation cell size is λ > π d = 170 mm. Assuming that the run-up distance to detonation $x_D = 500 \cdot \lambda$, the detonation cell size for stoichiometric hydrogen-air at cryogenic temperature T=101.7K is estimated to be λ = 9 mm and for 45%H2 the detonation cell size λ = 5 mm. Since the quasi-detonation has occurred, the detonation cell size for 20 and 50%H2 shouldn't be larger than the tube diameter ($\lambda_{max}$ = d = 54 mm)

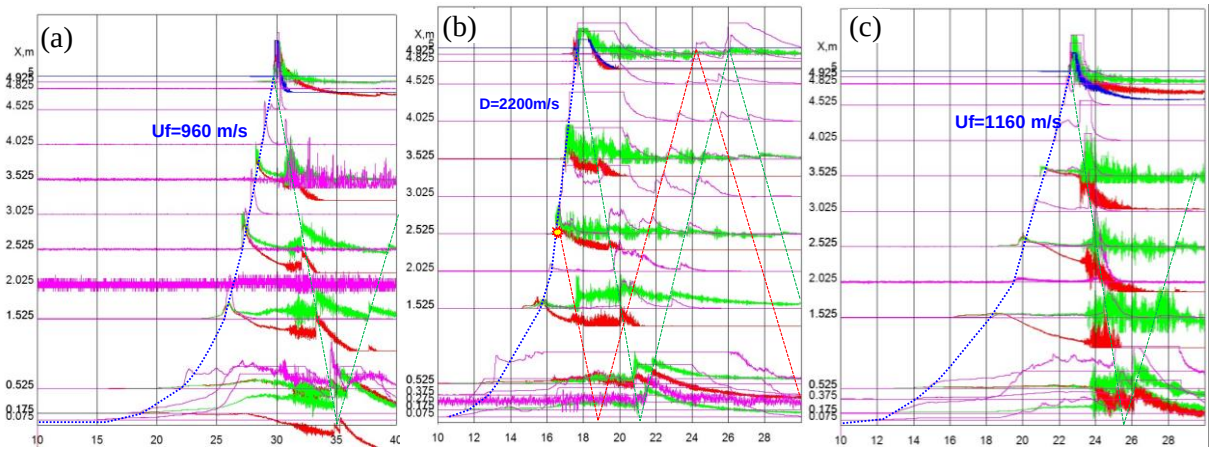


Figure 13. Distance-time diagram: (a) sonic deflagration of 19.9%$H_2$ (T=99.6K); (b) detonation transition of 45%$H_2$ (T=106K); (c) sonic deflagration of 50%$H_2$ (T=102K): flame trajectory (blue dotted line); light signal (pink solid line); pressure signal (red and green solid lines); shock wave trajectory (green dashed line).

Figure 14 shows a comparison of flame velocity for warm and cold experiments for different regimes of flame propagation. The figure shows that cryogenic temperatures promote the sonic flame propagation or even quasi-detonation for lean (20%H2) and rich (50%H2) hydrogen-air mixtures in comparison with ambient temperature combustion with a velocity below 80 m/s. For more reactive mixtures with 29 and 45% H2-air, cryogenic temperatures shorten the run-up distance to detonation compared to ambient temperatures.

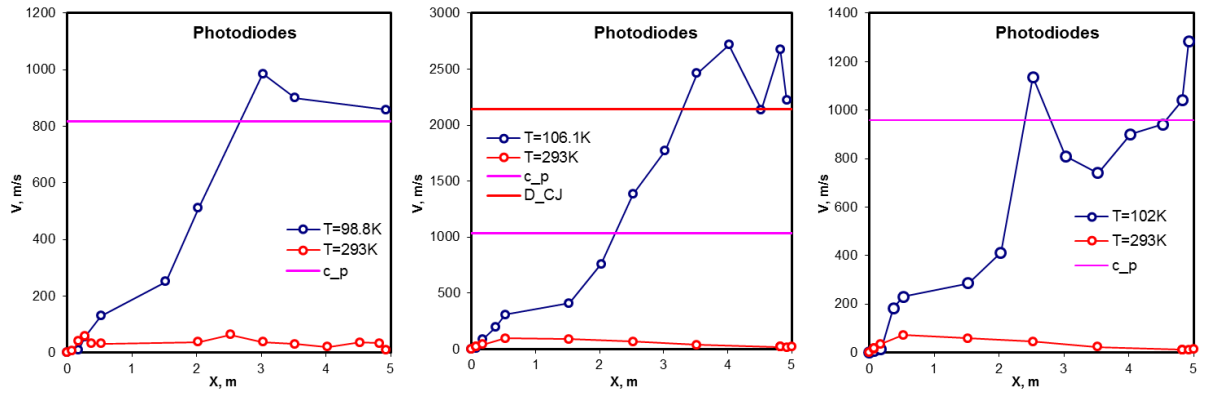


Figure 14. Comparison of flame velocity in smooth tube (BR=0%) at cryogenic and ambient temperatures: c_p and D_CJ are the speed of sound in combustion products and detonation velocity at the initial cryogenic temperature: 20% H2-air (left); 45% H2-air (centre), 50%H2-air (right).

This might be due to more efficient flame acceleration in more viscous and dense gas at cryogenic temperatures. Chemical reactivity cannot be higher at cryogenic temperature because the 5 times lower laminar flame speed at cryogenic temperature 100K cannot be compensated by 3 times higher density and expansion ratio of combustion products. However, it can be compensated by 2 times lower speed of sound at cryogenic temperatures because it leads to two times higher dynamic pressure for the same flow/flame velocity. Thus, it remains only gas dynamic properties responsible for the faster flame acceleration at cryogenic temperatures. For instance, due to 7.5 times higher kinematic viscosity at ambient conditions compared to cryogenic temperature T=100K, the Reynolds number at cryogenic temperatures might be 5 times higher to reach the same threshold velocity for sonic deflagration. It promotes creation of turbulent flow ahead of the flame, which leads to additional flame acceleration to sonic deflagration.

Figure 19 distinguishes the critical expansion ratio σ*=12.5 for hydrogen-air mixtures at cryogenic temperatures. For hydrogen concentration above 16%H2 (σ=11.9) characteristic flame velocity is above the speed of sound in reactants $c_r$ (blue dotted line in Figure 15, right) and characteristic combustion pressure is above the adiabatic combustion pressure ΔPicc (red dotted line in Figure 15, left). Similar to warm tests, for more reactive mixtures the velocity establishes at the level of the speed of sound in combustion products $c_p$ typical for chocked flames in congested areas when the detonation transition is suppressed by the detonation cell size larger than the orifice diameter, λ > d=45.2 mm for BR = 0.3, according to papers [2,5-6,14]. The same flame acceleration threshold σ*=12.5 was found for BR=0.6 with the difference that the critical detonation cell size is λ < d/3=9.5 mm.

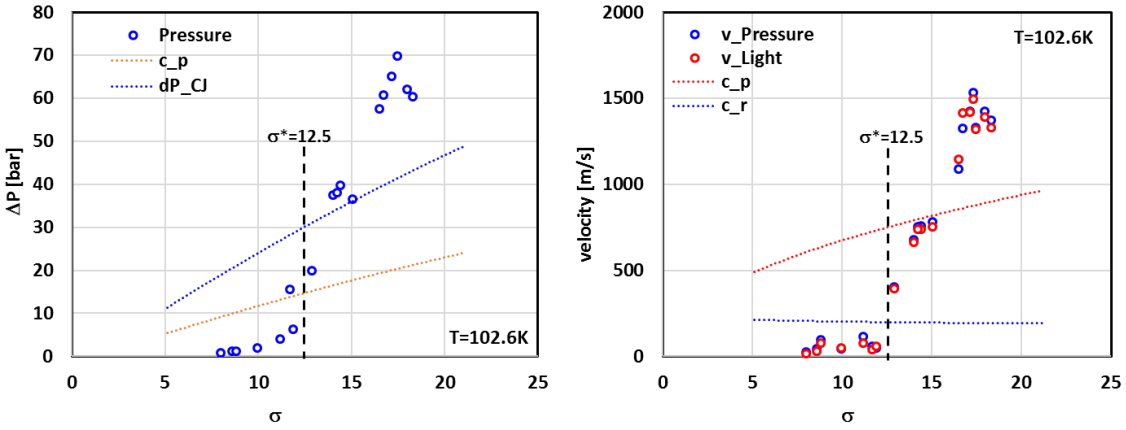


Figure 15. Experimental characteristic pressure (left) and flame velocity (right) as function of expansion ratio in obstructed tube (BR=0.3) at cryogenic temperature (T=102.6K): black dashed line is a cut-off line at σ*=12.5.

## 3.0 DISCUSSION

This chapter is dedicated to the analysis of all experimental data with respect to develop the criteria for effective flame acceleration and detonation transition which can be used to assess the hazard of cryogenic hydrogen combustion and for safety distances evaluation for humans and structures.

Integral combustion characteristics are the maximum combustion pressure and characteristic flame propagation velocity established in the main combustion process. Based on gas dynamic relationship and considering the flame as a piston for shock wave propagation, there is a dependence of dynamic pressure against the flow velocity:

$$\frac{P_2}{P_1} = \frac{2\gamma}{\gamma+1} M^2 - \frac{\gamma-1}{\gamma+1} \qquad (3)$$

where $P_2$ is the dynamic combustion pressure in our case; $P_1$ is the initial pressure 1 bar; γ is the adiabatic coefficient of burned composition; M = v/c is the Mach number as a ratio of flow (fame) velocity v = Uf over the speed of sound reactants c = cr. Figure 16 shows a comparison of dynamic pressure at cryogenic temperature T = 100K and ambient temperature for the same stoichiometric hydrogen-air mixture. It shows that dynamic pressure at cryogenic temperature is 2-3 times higher than that at ambient temperature for the same flow velocity. The reasons are almost two times lower speed of sound and larger adiabatic coefficient at cryogenic temperature. Such behaviour was experimentally confirmed in current experiments for different tube geometry (Figure 18). It was shown that the maximum combustion pressure at the temperature T = 100K is about 2 times higher than at ambient temperature. It is of practical interest that the dependence pressure vs. flame velocity

is linear. Theoretically, the overpressure of about 2.6 bar corresponds to the flow speed with the speed of sound (M = 1). This is the main reason to prevent fast sonic deflagration for safety applications.

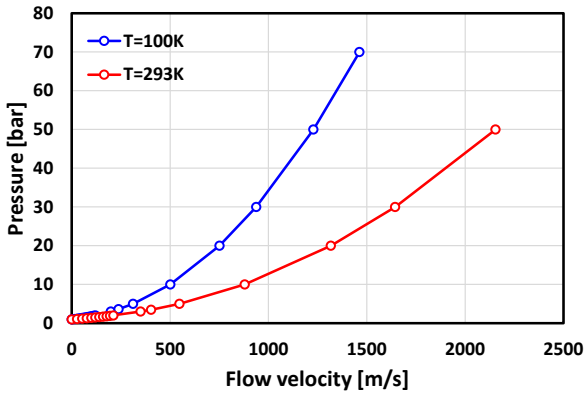


Figure 16. Dynamic pressure as a function of flow velocity calculated for stoichiometric hydrogen air at two different temperatures.

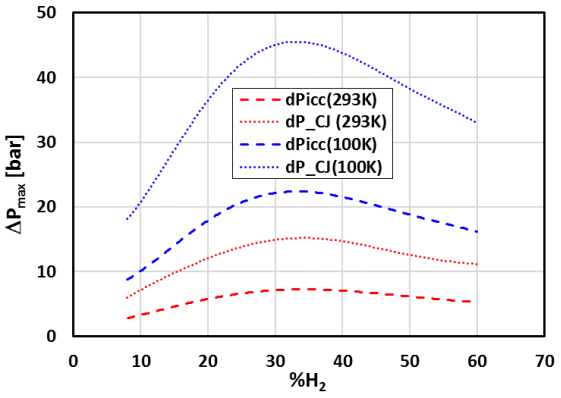


Figure 17. Theoretical maximum combustion pressure as function of hydrogen concentration at different initial temperatures.

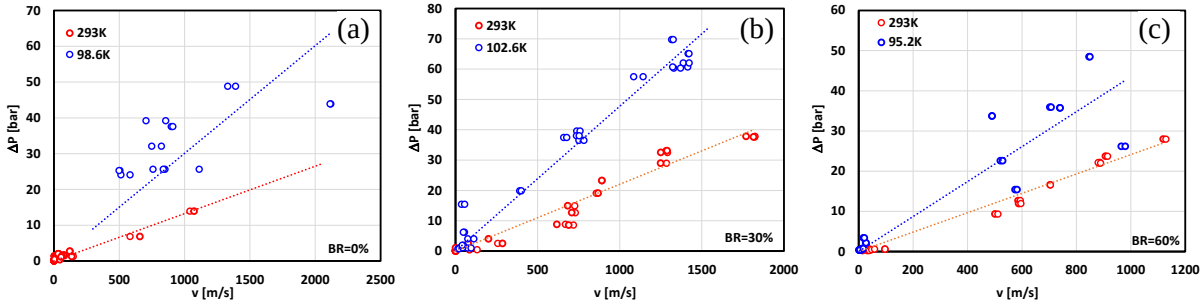


Figure 18. Maximum combustion pressure as function of characteristic flame velocity in obstructed and smooth tube: a) BR=0%; b) BR=30%; c) BR=60%.

Adiabatic combustion pressure demonstrates the same difference of maximum combustion pressure for sonic deflagration and detonation regimes for all combustible mixtures (Figure 17) The figure shows that even sonic deflagration produces the pressure 3 times higher than that at ambient initial temperature and exceeds 1.5 times the detonation pressure at the ambient initial temperature. The maximum combustion pressures at cryogenic temperature P(T) can be calculated from the reference data at ambient conditions $P(T_0)$ times the temperature factor:

$$P_{icc}(T) = P_{icc}(T_0)\cdot\left(\frac{T_0}{T}\right) \quad (4)$$

$$P_{CJ}(T) = P_{CJ}(T_0)\cdot\left(\frac{T_0}{T}\right) \quad (5)$$

where Picc(T) and $P_{CJ}(T)$ are the adiabatic combustion pressure and Chapman-Jouguet detonation pressure for a certain hydrogen concentration. This means that cryogenic hydrogen combustion is much more dangerous than detonation at ambient temperature. To prevent such a dangerous development of the combustion process with very high combustion pressure the flame velocity shouldn't exceed the speed of sound in reactants (M <1). As we found, the criterion for such a scenario is the critical expansion ratio shouldn't be exceeded by the value for the tested combustible mixture $\sigma < \sigma^*$ ($\sigma^*$= 12.5 at T=100K). Figure 19 summarizes all experimental data of current work with an

extension to evaluated temperature T = 650K from the paper [1]. So that it covers the temperature range from cryogenic T = 90K to elevated temperature T = 650K. Open points show current experimental data on expansion ratios at different temperatures. With a good accuracy the border line between slow (M<1) and fast sonic deflagration (M>1) can be approximated by exponential dependence on initial temperature T[K]:

$$\sigma^* = 2200 \cdot T^{-1.12} \tag{6}$$

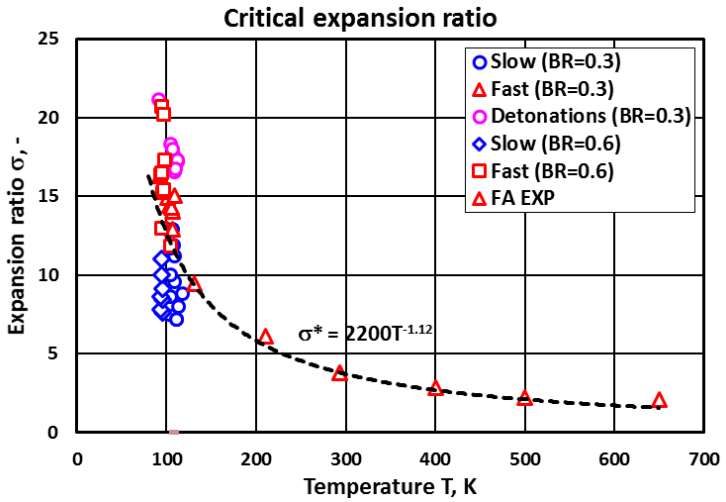


Figure 19. Critical expansion ratio as function of initial temperature based on experiments in obstructed tubes (BR=0.3 and BR=0.6): black dashed line is the border between slow and fast flames.

The cut-off line for fast and slow deflagration described by equation Eq. (6) is very close to hyperbolic dependence on initial temperature. We may transform it as follows

$$\sigma^*(T) = \sigma^*(T_0) \cdot \left( \frac{T_0}{T} \right) \tag{7}$$

where $\sigma^*(T_0)$ = 3.75 at the ambient temperature $T_0$ = 293K. Then, for T = 100K we get more conservative values of $\sigma^*(T)$ = 11.0 instead of $\sigma^*(T)$ = 12.6 according to Eq. (4). Still, the Eq. (7) is very valuable for the prediction of flame acceleration limits at different temperatures.

The next limits we found in current work at cryogenic temperatures are the detonability limits based on detonation cell sizes. Since we did not directly measure the detonation cell sizes at cryogenic temperatures, we used existing detonability limits for detonation cell size evaluation:

$$d > \lambda / \pi \quad \text{for detonation propagation in a smooth tube (BR = 0)} \tag{8}$$

$$X_D < 500 \cdot \lambda \quad \text{for run-up-distance in a smooth tube (BR = 0)} \tag{9}$$

$$d > \lambda \quad \text{for detonation propagation in an obstructed tube (BR = 0.3)} \tag{10}$$

$$d > 3 \cdot \lambda \quad \text{for detonation propagation in an obstructed tube (BR = 0.6)} \tag{11}$$

where d is the characteristic diameter of the system: d = D a tube diameter for smooth tube; d = d an orifice size for the obstructed tube with BR = 0.3 and BR = 0.6; $X_D$ is the run-up-distance to detonation in a smooth tube. The most crucial limitation is given by Eq. (8) as λ < 170 mm, as the maximum detonation cell size for detonable mixtures in a tube of 54 mm diameter. This means that the mixtures with λ > 170 mm cannot detonate in our tube at all. All the criteria for detonation onset have been checked at ambient temperature with known detonation cell sizes. Then the criteria were

extrapolated to cryogenic temperatures. All the limitations for detonation onset at cryogenic temperatures are put to Figure 20. The figure shows some difference in detonation cell sizes at cryogenic and ambient temperature but much less than expected in our predictions. The data for detonation cell sizes can be approximated as polynomial dependence on hydrogen concentration:

$$\lambda = 0.0006724[H_2]^4 - 0.1039[H_2]^3 + 6.0786[H_2]^2 - 159.74[H_2] + 1603.3 \qquad (12)$$

where $[H_2]$ is the hydrogen concentration in molar percent.

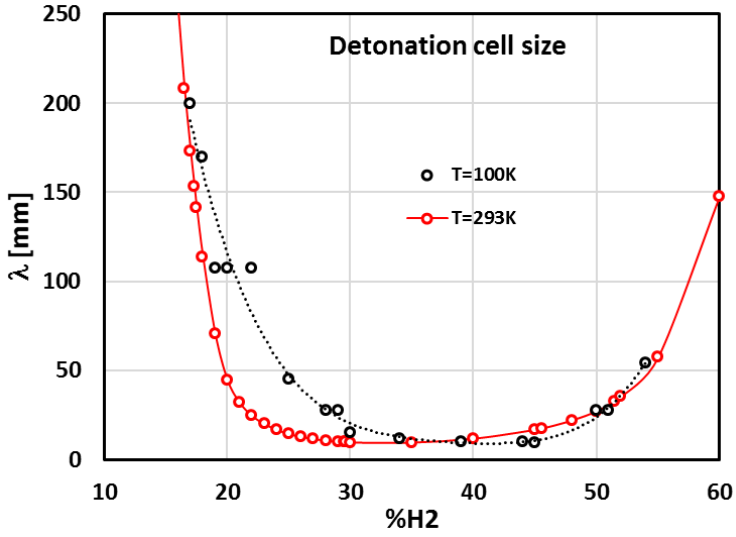


Figure 20. Detonation cell size derived by existing detonability limits at cryogenic temperature T=100K in comparison with the data at ambient temperature T = 293K.

## 4.0 SUMMARY, CONCLUSIONS AND OUTLOOK

In the frame of the PRESLHY project, more than 100 experiments were made with the Cryogenic Shock Tube facility at HYKA KIT. About half of the experiments was made at cryogenic temperatures (from 80 to 130 K). During the experimental campaign, many difficulties were encountered as temperature nonuniformity, condensation of the mixture, ignition problems approaching the flammability limits, flame visualization and some others. It turned out to be impossible to ignite even hydrogen-rich mixtures at 77 K and it was not possible to achieve uniform temperatures along the tube at higher (approx. 150 K) temperatures. The photo sensors turned out to be too insensitive for slower combustion processes with less intensive radiation. However, all the problems were satisfactory solved and the flame propagations regimes at cryogenic temperatures were found.

The critical conditions for flame acceleration were evaluated as a function of initial temperature within the range 90 – 650K. It shows a much higher hydrogen concentration leading to sonic deflagration than was predicted by advanced extrapolation before the tests. The correlation based on current experiments is quite simple and useful:

$$\sigma^* = 2200 \cdot T^{-1.12}$$

The detonation cell sizes at cryogenic temperature T = 100K are evaluated on the basis of existing criteria for detonation onset in smooth and obstructed tubes and can be presented as a polynomial function of hydrogen concentration [H2]:

$$\lambda[\text{mm}] = 0.0006724[H_2]^4 - 0.1039[H_2]^3 + 6.0786[H_2]^2 - 159.74[H_2] + 1603.3$$

Based on evaluated detonation cell size the well known criteria can be used to assess the detonability of hydrogen –air mixtures at cryogenic temperatures in different geometries and scales.

The run-up distance to detonation at cryogenic temperatures was found to be two times shorter than at ambient temperature. For the first time in a smooth channel, a steady-state flame propagation with the speed of sound in combustion products was registered for a long distance.

It was found that the maximum combustion pressure at cryogenic temperatures is 2-3 times higher than that for ambient conditions. It demonstrates a high level of the danger under cryogenic hydrogen combustion. Theoretically, even adiabatic combustion pressure corresponding to sonic deflagration at cryogenic temperature is 1.5 times higher than the CJ-detonation pressure at ambient temperature.

All the data and criteria can be used for RCS recommendations and safety distance evaluations. Original experimental data will be valuable for numerical code validation as well.

**REFERENCES**


1. Dorofeev, S.B., Kuznetsov, M.S., Alekseev, V.I., Efimenko, A.A., Breitung, W. (2001) Evaluation of limits for effective flame acceleration in hydrogen mixtures. *J. Loss Prev. Proc. Ind*., 14 (6): 583-589.
2. Dorofeev, S.B., Sidorov, V. P., Kuznetsov, M. S., Matsukov, I. D., Alekseev, V. I. (2000) Effect of scale on the onset of detonations. *Shock Waves*, v. 10, pp. 137-149.
3. Kuznetsov, M., Alekseev, V., Matsukov, I., Dorofeev, S. (2005) DDT in a smooth tube filled with a hydrogen–oxygen mixture. *Shock Waves*, 14: 205-215.
4. Ciccarelli, G., Dorofeev, S. Flame acceleration and transition to detonation in ducts, *Progress in Energy and Combustion Science*, Volume 34, Issue 4, 2008, Pages 499-550
5. Kuznetsov, M.S., Alekseev, V. I., Dorofeev, S. B. (2000) Comparison of critical conditions for DDT in regular and irregular cellular detonation systems. *Shock Waves*, v. 10, pp. 217-224.
6. Teodorczyk, A., Lee, J.H., Knystautas, R. (1988) Propagation mechanism of quasi-detonations. *22nd Symposium (Int.) on Combustion*. The Combustion Institute, Pittsburgh, pp 1723–1731.
7. Zitoun, R., D. Desbordes, C. Guerraud, and B. Deshaies. Direct initiation of detonation in cryogenic gaseous H_2-O_2 mixtures. Shock Waves, 4(6):331-337, 1995.
8. Stamps D.W. and S.R. Tieszen. The influence of initial pressure and temperature on hydrogen-air-diluent detonations. *Combust. Flame*, 83(3):353-364, 1991.
9. Tieszen, S.R., M.P. Sherman, W.B. Benedick, and M. Berman. Detonability of H2-air-diluent mixtures. Technical Report NUREG/CR-4905, SAND85-1263, Sandia National Laboratories, 1987.
10. Denisov, Yu.N. and Ya.K. Troshin. Structure of gaseous detonation in tubes. *Sov. Phys. Tech. Phys*., 5(4):419-431, 1960.
11. Gavrikov, A.I., Efimenko, A.A., Dorofeev, S.B (2000) A model for detonation cell size prediction from chemical kinetics. *Combustion and Flame*, 120 (1-2): 19-33.
12. Reynolds, W.C., The element potential method for chemical equilibrium analysis: implementation in the interactive program STANJAN, Stanford University, Stanford, CA, 1986
13. Goodwin, D., Cantera: An object-oriented software toolkit for chemical kinetics, thermodynamics, and transport processes, Caltech, Pasadena, 2009.
14. Lee JH, Knystautas R, Chan CK (1984) Turbulent flame propagation in obstacle-filled tubes. 20th Symposium (Int.) on Combustion, The Combustion Institute, Pittsburgh, PA, pp 1663–1672